Hydrogen storage mechanism and lithium dynamics in $Li_{12}C_{60}$ investigated by μSR

Authors: Mattia Gaboardi[1], Chiara Cavallari[1,2], Giacomo Magnani[1], Daniele Pontiroli[1], Stephane Rols[2], Mauro Riccò[1,*]

1. *Dipartimento di Fisica e Scienze della Terra, Università degli Studi di Parma, Parco Area delle Scienze 7/a, 43124 Parma, Italy.*
2. *Institut Laue-Langevin (ILL), 71 avenue des Martyrs CS 20156, F - 38042 Grenoble Cedex 9.*

Abstract: The lithium cluster intercalated fulleride $Li_{12}C_{60}$ was investigated by means of Muon Spin Relaxation (μSR) spectroscopy with the intent of unveil its hydrogen storage mechanism. Thanks to the well-known propensity of positive muons to form Muonium, a light isotope of the hydrogen atom, the final stages of the absorption process can be probed. The appearance of a slow oscillating signal in the time evolution of the muon polarization indicates the presence of Li-Mu covalent pair, never observed before in lower doped Li fullerides, which mimics the formation of LiH at the first stage of hydrogen chemisorption in the material. In addition, the μSR signal shows a clear transition above 150 K, compatible with a thermally activated Li cluster rearrangement. The combined Inelastic Neutron Scattering analysis suggests that tetrahedral Li clusters may undergo a progressive melting upon heating, which could favour room temperature ionic diffusion.

1. Introduction

In the last decades, hydrogen has gained a great technological interest as possible replacement of fossil fuels. However, one of the main drawback for the development of a hydrogen economy is represented by the difficulties of storing hydrogen in an efficient way [1]. In the wide panorama of solid-state hydrogen storage systems, carbon based materials are especially suitable because of the low weight and cost of carbon [2]. In particular, metal decorated fullerenes appear an intriguing family of compounds, as it was predicted that high amounts of molecular hydrogen can be absorbed with a reasonable binding energy, suitable for technological applications [3–5]. Unfortunately, the existence of such superulleroids systems in the solid-state has never been confirmed, mainly due to the marked tendency of metals towards clusterization [6]. Nonetheless, the intercalation of lithium and sodium at high extent in fullerene host lattice leads to the formation of alkali-cluster intercalated fullerides, which indeed proved to reversibly uptake rather high amount of hydrogen

*Email: mauro.ricco@fis.unipr.it

via a complex chemisorption mechanism [7–10]. In these systems, the number of intercalated ions equals or exceeds the six-fold degeneracy of the t_{1u}-LUMO of C_{60}. Under this condition, fullerene is charged with six electrons and the remaining electrons are forced to stay on the metal cluster. We found that in these systems hydrogen mainly covalently binds to the C_{60} molecule, thus forming the so-called hydrofullerene ($C_{60}H_y$, y ~ 36-48), while a minority part reacts with a fraction of the alkali metal ion (Li or Na), segregating as alkali hydride. From a structural point of view, in the starting material the alkali cluster is placed in the octahedral [11–13] or tetrahedral [14] voids of the parent *fcc* fullerite structure, while the finally obtained hydrogenated system is characterized by the high steric hindrance of $C_{60}H_y$ (packed in a *bcc* or highly expanded *fcc* lattice) which allows only few metal ions to be retained in the structure. Although the study of the starting and the final products are relatively straightforward, the intermediate hydrogenation steps are not yet fully understood. Muon Spin Relaxation (μSR) already revealed part of this mechanism on Li_6C_{60} and $Na_{10}C_{60}$ [15], in this work we will show, however, that in $Li_{12}C_{60}$ this process looks quite different. μSR spectroscopy is a well suited technique to study hydrogen storage materials thanks to the chemical similarity shared by a hydrogen atom and Muonium. In fact, muons (μ^+) are particles with ½ nuclear spin and 1/9 of the proton mass. Similarly to protons, when implanted in low density charge carriers compounds, they can bind to an electron and form muonium (Mu), a light isotope of atomic hydrogen. This ability makes μSR a unique tool for studying the behaviour of a single hydrogen atom in matter. In Li_6C_{60} and $Na_{10}C_{60,}$ the hydrogen molecule undergoes an initial dissociation operated by the intercalated partly ionized alkali clusters. Subsequently, the hydrogen atoms are covalently bound to the C_{60}^{6-} anions. In this case, the μSR experiment has shown a high fraction of μ^+ forming Mu which quickly react with C_{60}^{6-}, producing C_{60}-Mu adduct radicals [15]. This fraction increases if temperature is lowered, indicating that the reaction between C_{60} and atomic hydrogen occurs with a very low energy barrier. This observation clarified that the relatively high temperatures (T > 373 K) needed to start the H_2 absorption [7,8] are then required only to activate the H_2 dissociation process operated by the alkali cluster.

The ability of Li to form clusters when intercalated in C_{60} is well documented [13,14,16,17]. At low temperature (20 K), $Li_{12}C_{60}$ is a monoclinic crystal (space group $P2_1/c$; a = 9.888(9) Å, b = 9.901(8) Å, c = 14.290(8) Å, β = 89.51(6)°) where the C_{60} molecules are centred in the same way of the *fcc* C_{60} structure, but rotated to ~ 90° around the [001] axis of the parent cubic lattice. This structure is characterized by the presence of a small cluster of five Li atoms (with a centred tetrahedron structure), residing in the pseudo-tetrahedral voids of the parent *fcc* lattice (see Figure1a), while the remaining two Li ions, which complete the stoichiometry, are delocalized in the remaining interstitial space.[14] Above 553 K the structure was determined to be *fcc* (space

group $Fm\bar{3}m$), with a Li cluster in the central octahedral void and the C_{60} molecule characterized by rotational disorder [17].

$Li_{12}C_{60}$ is able to reversibly absorb up to 5 mass% H_2 with an onset temperature below 373 K [10], about 150 K lower than Li_6C_{60} [7]. In both materials, after the absorption of hydrogen a partial segregation of LiH has been identified.

In this work, the interaction of $Li_{12}C_{60}$ with atomic hydrogen is investigated by means of μSR spectroscopy. We discovered here a new mechanism of hydrogenation, different from the one observed Li_6C_{60} and $Na_{10}C_{60}$ parent compounds. Moreover, the Li dynamics is probed by both μSR and Inelastic Neutron Scattering, revealing an internal Li cluster rearrangement, which suggests the activation of Li diffusion above 150 K.

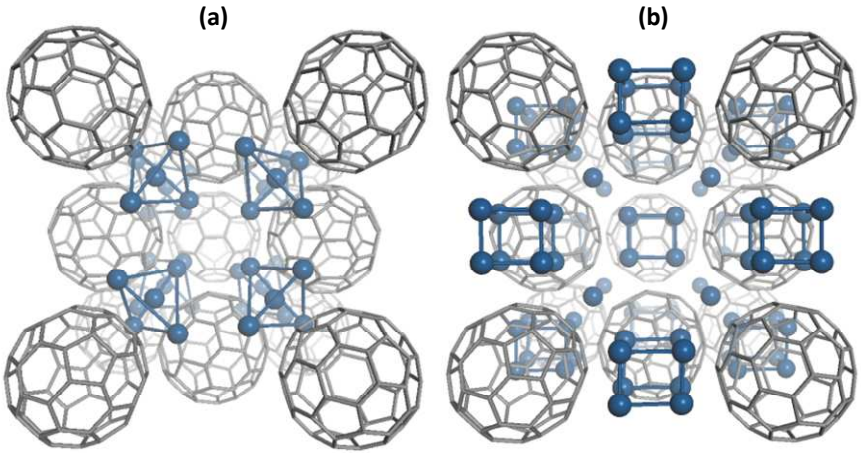

Figure 1: (a) Low temperature phase of $Li_{12}C_{60}$ [14]*. (b) High temperature phase as suggested by μSR and INS experiments (as explained in results and discussion paragraph). The C_{60} in the foreground has been omitted for clarity.*

2. Experimental

The $Li_{12}C_{60}$ crystalline powder was synthesized as described in reference [14] by cutting small pieces of lithium (Sigma Aldrich, 99 %) and mixing them with C_{60} powder (MER Corp., 99.9 %) in stoichiometric amount. The μSR experiment was carried out on the Argus spectrometer at ISIS-Rutherford Appleton laboratory (Didcot, UK) at the RIKEN-RAL Muon facility. The 100% spin-polarized pulsed beam of this facility is optimized to study the muon spin evolution over long time-scales. About 350 mg of $Li_{12}C_{60}$ was pressed and sealed in an air-tight silver-coated aluminium cell, capped by a kapton window. The total experimental muon polarization asymmetry was established to be 21.10(15)%, estimated on a separate transverse field (TF) experiment on pure silver. The baseline, due to muons stopping outside the sample, is measured to be 5.76(11)% of the total

polarization. The muon polarization is followed by plotting the asymmetry function, expressed as $A(t) = [N_b(t) - \alpha N_f(t)]/[N_b(t) + \alpha N_f(t)]$, where $N_{b/f}$ is the backward/forward collected counts and α is a geometrical parameter, calibrated for each temperature by fitting the oscillation observed under the application of a 20 G transversal field (TF). Data were analysed by means of the WiMDA software [18], after correcting for the double–pulsed structure of the muon beam.

Magnetic measurements (shown in Supplementary Information) were performed on a Quantum Design XPMSXL-5 SQuID magnetometer, in the temperature range 2-300 K and field range 0-5 T. The Zero Field Cooling (ZFC) and Field Cooling (FC) experiments were recorded in an applied magnetic field of 3 T. Density Functional Theory (DFT) calculations were carried out by means of DMol3 code [19], within the generalized gradient approximation (GGA), in the formulation by Perdew Burke Ernzerhof (PBE functional) [20] and using a DNP basis set. The molecule was relaxed until the maximum force acting on each atoms was less than 0.002 Ha/Å and then the quadrupolar tensor was calculated on different nucleus. Inelastic Neutron Scattering (INS) measurements have been carried out on the thermal neutrons time-of-flight spectrometer IN4C at the ILL, in Grenoble, France. About 300 mg of $Li_{12}C_{60}$ powder has been sealed in an aluminium flat container sealed with an indium o-ring and measured using neutron incident wavelengths of 1.11 and 2.41 Å. This allowed us to probe the dynamics either in Stokes or in the anti-Stokes side, covering different energy ranges with different resolutions. The measurements, performed at different temperatures from 10 to 320 K, have been normalized to the monitor counts, the vanadium standard and then corrected for the background and the scattering coming from the sample holder. The signal was then converted into the so-called generalized density of states $GDOS(\omega, T)$ [21]. The theoretical $G(\omega, T)$ has been calculated on the basis of first-principles calculations, performed using the projector augmented wave (PAW) formalism [22] of the Kohn-Sham density functional theory, within the generalized gradient approximation (GGA) [20], as implemented in the Vienna ab-initio simulation package (VASP) [23]. All electronic functions have been calculated at the gamma point only and an energy cut-off of 450.0 eV was used. Geometry relaxation and a series of single point energy calculations were carried out on $Li_{12}C_{60}$ structural unit as reported in literature [14]. Phonons have been extracted using the direct method as implemented in the Phonon software [24]. $G(\omega, T, Q)$ has been calculated from the partial density of states $g_i(\omega)$ as:

$$G(\omega, T, Q) = \sum_{i=1}^{N} \frac{\sigma_i(coh)+\sigma_i(inc)}{m_i} g_i(\omega) e^{-2W_i(Q)}.$$

Where $\sigma_i(coh)$ and $\sigma_i(inc)$ indicate the coherent and incoherent cross section respectively, m_i is the mass and $W_i(Q)$ is the Debye-Waller factor for the atom i. Finally, the summation $G^{th}(\omega, T) = \int G(\omega, T, Q) dQ$ has been carried out on a regular Q-grid, matching the Q-space covered by the experiment. The calculated spectra, convoluted with the experimental resolution function, were then

compared to the experimental data. As we will discuss into the discussion section and in the Supplementary Information, the combination of appropriate simulations and INS experiments are of crucial importance for getting a deep insight into the dynamical properties of materials.

3. Results and discussion

The zero field (ZF) time evolution of the muon polarization of $Li_{12}C_{60}$ is displayed, for different temperatures, in Figure 2. A remarkable difference is immediately evident with respect to the previously studied cluster-intercalated fullerides (Li_6C_{60} and $Na_{10}C_{60}$) [15]: the initial polarization of $Li_{12}C_{60}$ is 100% of the total asymmetry, while in the previous cases a sizeable missing fraction was present. This despite the fact that $Li_{12}C_{60}$ shows similar hydrogen absorption features as compared with the other fullerides. In Li_6C_{60} and $Na_{10}C_{60}$, the large fraction of the missing initial polarisation was attributed to the formation of radical species on the negatively charged fullerene molecule. In this case, the strong hyperfine coupling between the μ^+ and the nearby radical electron generate a muon precession frequency that exceeds the pass band of the instrument. However, the application of a longitudinal field (LF) allowed to repolarize this missing fraction and to estimate the value of the muon-electron hyperfine coupling [15].

In $Li_{12}C_{60}$, the absence of missing fraction suggests that no radical is formed on C_{60}^{6-}, probably because some more efficient processes prevail in the Mu reaction pathway. Moreover, the ZF relaxation observed in $Li_{12}C_{60}$ is also different from the Li_6C_{60} case, where a simple lorentzian decay was observed and easily ascribed to interstitial μ^+ diffusion. Due to the low natural abundance of ^{13}C (~1%) and to the diamagnetic nature of these material, as indicated by SQUID investigation (see Supporting Information, Fig. SI1), the only possible spin interaction which the muon experiences is the eteronuclear dipolar coupling with ^7Li nuclear spins (I = 3/2; the 7% natural abundance of ^6Li gives a negligible contribution). As shown in Figure 2, the complex ZF relaxation observed in $Li_{12}C_{60}$ can be properly fitted with two different components: 1- a Gaussian decaying component and 2- a slowly oscillating component.

1- The former can originate from a multiple dipolar spin interaction. This would in principle induce a static Kubo-Toyabe (K-T) decay of the muon polarization [25], however, the short time portion of this decay can be well approximated by a Gaussian function. The 1/3 recovery expected for the K-T decay would, in our case, fall outside the experimental time window. The Gaussian decaying part of the polarization can be fitted with the function:

$$P_G(\Delta, t) = A_G exp\left(-\frac{1}{2}\gamma_\mu^2 \Delta^2 t^2\right), \quad (1)$$

where γ_μ is the muon gyromagnetic ratio and Δ is related to the dipolar interaction through the

function [26]:

$$\Delta^2 = \frac{8}{9} I(I+1)\hbar^2 \gamma_{Li}^2 F \sum_{j=1}^{N} r_j^{-6} , \qquad (2)$$

where F = 1 for integer spins and it is $1 + \frac{3}{8}\frac{I+1/2}{I(I+1)}$ for odd half-integer spins while r_j is the distance between the muon and the j-th nucleus [26,27]. Equation 1 describes the time evolution of the spin of those muons stopped interstitially or substitutionally to the metal, thus probing the nuclear dipolar field of the many Li ions intercalated in the lattice. Incidentally, since ^{7}Li nucleus has a non-zero quadrupolar moment, the spin Hamiltonian will contain a quadrupolar term in addition to the dipolar one. In case of few N neighbouring nuclei, one has to solve the $2(2I+1)^N$ dimensional problem, while, if N is high enough, as in our case, the K-T or Gaussian relaxations become again a good approximation and the previously adopted approach is fully justified [28].

2- Evidently, this is not the case for the second slowly oscillating component, which cannot be properly fitted by a K-T function (either static or dynamic [25]), especially for the longer time part of the μSR histogram. On the other hand, a K-T fit of the oscillating part gives a large value for Δ (about 4.5 G, $\gamma_\mu \Delta \sim 0.4\,\mu s^{-1}$) corresponding to an average μ-^{7}Li distance incompatible with the structure of this compound (it would suggest an aggregation of ^{7}Li's around the muon, not likely if we take into account the positive charge of both). On the contrary, this part of the spin evolution can be fitted by a decaying oscillatory function.

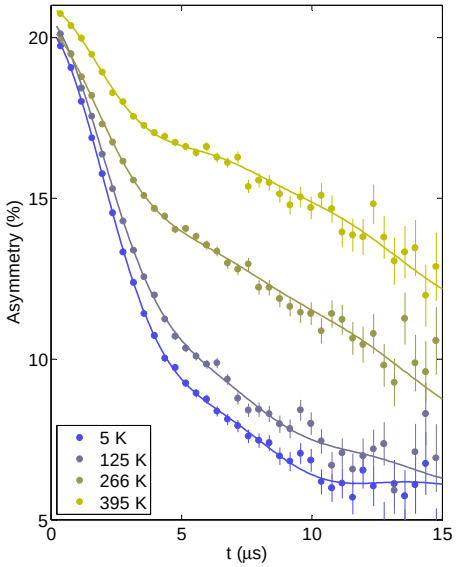

Figure 2: Zero Field μSR asymmetry spectra of $Li_{12}C_{60}$ for selected temperatures. Solid lines represent the fit to equation 3.

Such an oscillation could be originated either by a dipolar interaction of the muon with a single ^{7}Li nucleus sitting quite close to it, or by the hyperfine interaction of the muon with a long range ordered magnetic phase (hypothesis excluded by magnetometry measurements, as previously discussed). The interaction between the muon and a single lithium spin can be analytically modelled by considering the full Hamiltonian in terms of dipolar and quadrupolar coupling, as described by Meier [29]. The ZF asymmetries were fitted, for different temperatures, according to the function:

$$P_z(t) = P_M(\nu_D, \nu_Q, t)\exp(-\lambda t) + P_G(\Delta, \mathrm{t}). \qquad (3)$$

Here P_M is the Meier function, with ν_D and ν_Q respectively the dipolar and quadrupolar frequencies [29]. The observed lorentzian decay of the oscillation is attributed to the ^{7}Li diffusional and vibrational dynamics.

The fits with the above-described model are shown in Figure 2 and the results of the fits are displayed in Figure 3. All efforts aimed to adopt different models, for instance by replacing the oscillating term by a static K-T (or Gaussian) relaxation, worsen the fit and leads to non-physical results. In order to explain this result we have to make some considerations. As already observed in the parent systems Li_6C_{60} and $Na_{10}C_{60}$ [15], the partial electron charge residing on Li clusters can interact with the implanted μ^+ during the muon thermalization process, inducing the production of Mu. Moreover, the high negative charge owned by C_{60} (6 electrons) can easily leads the creation of a C_{60}-Mu adduct radical and it is also known to inhibit the formation of endohedral muonium (Mu@C_{60}, *e.g.:* a Mu residing at the centre of C_{60}) otherwise observed in other fullerides. However, neither a stable Mu atom nor a radical is formed in $Li_{12}C_{60}$, as no signature for the existence of a muon hyperfine interaction with a paramagnetic electron is observed. This, however, does not exclude that Mu is formed as precursor of an efficient process that can quickly trap it and leave the muon in a diamagnetic environment (i.e. no unpaired electrons are present around the muon). Other possibilities are that the muon does not trap any electron (although the slightly positive Li's are not expected to attract a bare μ^+) and sit interstitially or substitutionally to Li. Alternatively, two electrons could bind to the muon forming the muonium ion Mu^- (experimentally observed on LiH [30,31]). Following the latter hypothesis, if we assume the H^- radius and simulate the free volume accessible by it, only two distinct interstitial positions are large enough to accept it: the centre of the big pseudo-octahedral void (which at 20 K resulted unoccupied by Li ions, according to our recent structural study) [14] or the centre of the C_{60} molecule (Mu^-@C_{60}), as already observed by MacFarlane *et al.* [32]. For both these configurations, and for other possible locations within the $Li_{12}C_{60}$ structure, we calculated, from equation 2, the dipolar field (Δ) and we compared it with the Gaussian width of the fit displayed in Figure 3c. In Table 1, the average radius and calculated $\gamma_\mu\Delta$ are reported for different sterically allowed substitutional or interstitial sites. Since the values

reported in Table 1 were calculated for the structure refined at 20 K (reference [14]), we have to compare them with the experimental value of $\gamma_\mu\Delta$~0.2 μs^{-1} extrapolated at this temperature. By the comparison of the found values with the experimentally observed ones displayed in Figure 3c it is evident that the (a) case (μ^+ in the centre of the tetrahedral cluster) is the one that better reproduces the experimental values.

Table 1: Average distance $\langle R \rangle$ between muon and the first neighbour Li ions for allowed muon sites in $Li_{12}C_{60}$ structure [14]*, the relative number of first neighbour Li's and the calculated $\gamma_\mu\Delta$ from equation 2. a(b): one μ^+ substitutional to the Li ion at the centre (corner) of the Li_5 tetrahedral cluster. A muonium anion sitting at the centre of the cell (c) or endohedral (d). (e): a μ^+ replacing the tetrahedral Li ion in the high temperature phase of Fig.1b. (f): the Mu^- in LiH is also reported for comparison* [31].

Muon site	$\langle R \rangle$ (Å)	*first neighbour Li's*	Calculated $\gamma_\mu\Delta$ (μs^{-1})
[a)] μ^+@T_h-Li_5	2.7	4	0.20
[b)] μ^+ in T_h-Li_5 corner	4.07	7	0.10
[c)] Mu^-@O_h void	3.8	8	0.14
[d)] Mu^-@C_{60}	6.5	32	0.06
[e)] μ^+ in T_h void, O_h-Li_8 (HT phase)	3.7	4	0.07
[f)] Mu^- in LiH [31]	2.04	6	0.54

Following this discussion, below ~150 K the Gaussian relaxation can be attributed to the diamagnetic muons trapped in the centre of the tetrahedron, substitutional to the central Li. In this thermal range, $\gamma_\mu\Delta$ was calculated to vary between 0.25(2) (at 5 K) and 0.194(1) μs^{-1} (at 159 K). In fact, hydrogen is well known to easily cluster with alkali metals, and it is believed to hold a negative charge when added to neutral Li molecules [33]. In our case, it is difficult to assign a net charge on μ^+, since it becomes part of a charged molecule made of five lithium atoms, which should be thought as a whole. We can tentatively attribute a charge of two electrons per cluster (Li_5^{2+}), considering they are in number of two per C_{60} and two Li ions are disordered in the crystal. The average Li-H distance is about 1.6 Å for the covalent pair and may vary up to 1.85 Å in small clusters or molecules, while it is fixed to 2.04 Å in bulk lithium hydride salt [31].

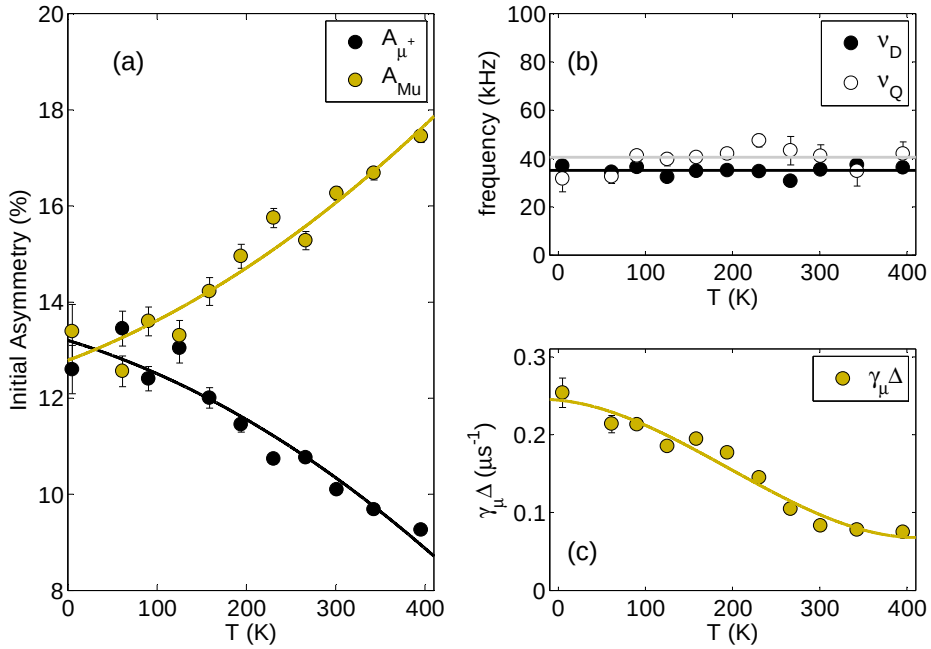

Figure 3: The results of the fit, according to equation 3, for the ZF-μSR data of $Li_{12}C_{60}$ displayed as a function of temperature. (a): amplitudes of the μ^+ (Gaussian) and LiMu (oscillating) components. (b): dipolar and quadrupolar frequencies of the LiMu oscillation (black and grey solid lines represents the respective average value). (c): relaxation rate ($\gamma_\mu \Delta$) of the Gaussian component. Solid lines in (a) and (c) are guides for the eyes.

Upon rising the temperature above 150 K, Δ considerably decreases, indicating a possible phase transition or the migration of the muon to another site, where the average distance between muon and lithium rises. In our opinion, the most plausible possibility is that the Li at the corners of the tetrahedron move far from the central ion toward the O_h void, raising the relative distance, thus forming a cubic cluster (Li_8^{4+}) in the larger central void of the cell, as observed by Cristofolini *et al* for Li_xC_{60} compounds (with $x \geq 12$) above 373 K [17]. The high temperature cluster configuration is depicted in Figure 1b. The muon, sitting at the centre of the low temperature tetrahedron, would maintain the same coordination and the dipolar field would decrease as far as the lithia at the corners move toward the centre of the cell. This hypothesis was taken into account by inverting equation 2 for $N = 4$ (the number of lithia at the cluster's corners) and substituting r_j by the average radius $\langle R \rangle$. The relative μ^+-Li distance is plotted in Figure 4, as a function of temperature, showing a gradual increase from ~2.5 to about 3.7 Å. In this condition, the cubic cluster at high temperature would have an average edge of about 2.6 Å (calculated from the cell at 20 K).

This hypothesis is confirmed by Inelastic Neutron Scattering (INS) investigations, which shows an evident temperature evolution of the spectral features associated to lithium cluster vibrations just around 250 K (see Figure 5).

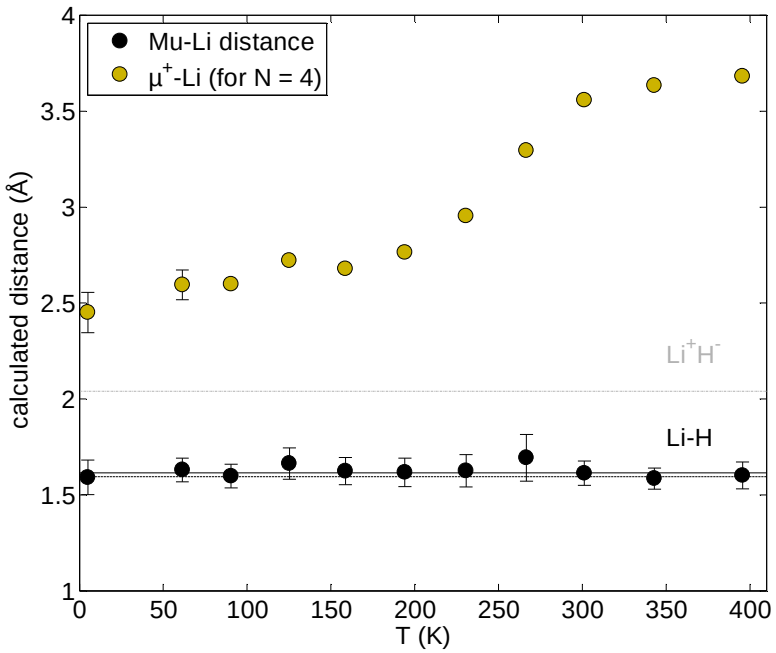

Figure 4: Black dots: distances extracted from the fit to equation 3 for the first LiMu oscillating component as a function of temperature. Dot-dashed lines represent the tabulated distances for the LiH covalent (black) and ionic (grey) bonds. The solid line is the average value of the fit. Yellow dots: Li-μ^+ average distance as computed from Δ for a coordination number of four Li (N=4), reported as a function of temperature.

In Figure 5 the GDOS of $Li_{12}C_{60}$ derived from IN4c measurements using 1.1 Å wavelength incident neutrons at 10, 200, 250 and 320 K is displayed. As clearly shown, the INS bands located around 15 and 22 meV (indicated by stars) drop as the temperature increases, while the other bands are essentially unaffected. The shaded area below 5 meV indicates the region where a strong contribution from the elastic line is present, hence it was not taken into account in our study. These data are compared to the Li and C partial GDOS calculated at 10 K. The partial GDOS of Li dominates the total spectrum in the "C_{60} gap" region, i.e. 10-27 meV, where no contribution from C vibrations is expected. In particular, the two peaks at 15 and 22 meV are in good agreement with those found in the experimental data. They were associated to vibrations involving Li atoms located at the corners of the tetrahedral Li cluster, while the central atom (navy area in Figure 5) contributes only weakly in this frequency range. These observations are compatible with a progressive melting of the Li- tetrahedral cluster upon heating. The lack of evolution of the principal C_{60} molecular

modes with temperature suggests the absence of severe modification of their local environment (see also Supporting Informations). The amplitude and temperature dependence of the observed μSR Gaussian decay can thus be reasonably explained by assuming that the muon stops inside the tetrahedral Li clusters and probes the $Li_{12}C_{60}$ structural phase transition.

Let's now move to the oscillatory muon fraction. As we explained above, the dipolar interaction of the muon with a single Li ion is responsible for the observed oscillating component. In analogy of what is observed for H, the muonium could form a Li^+Mu^- ionic pair (similarly to LiH) or a covalently bound Li-Mu molecule [33]. In both cases, the hyperfine coupling would be quenched by a singlet electronic state. In fact, in Li^+Mu^- the 2 electrons on μ^+ would fill the $1s$ hydrogenoid level, while in Mu-Li the electron on μ^+ and the one on Li would lower their energies by forming a bonding molecular orbital. The fit of the ZF polarization to equation 3 leads to ν_D = 35(2) kHz and ν_Q = 41(3) kHz (see Figure 3). The dipolar frequency is consistent with the formation of a single Li-Mu covalent bond, being the relative average extrapolated distance 1.62(7) Å and the Li-H covalent bond 1.599 Å [33]. The fit of the data at different temperatures show that the second oscillating component does not show any temperature dependence (see Figure 3b), suggesting the formation of a rather stable species. The lithium intended to form this bond is possibly one of the four at the corners of the T_h cluster or one of the two lithia delocalized in the lattice. Moreover, Figure 3a shows a clear temperature evolution of the μ^+ and Mu μSR amplitudes. While at 5 K the two species are present with the same fraction, at 400 K the percentage of muons covalently bound to Li decreases to ~33.5%. This may be compatible with the cluster expansion, also probed by INS, whose increasing sterical hindrance could inhibit the formation of Li-Mu covalent bond.

Furthermore, the quadrupolar frequency is also in good agreement with the DFT calculation made on an isolated covalent Li-H. In this case it results ν_Q = 46 kHz, for a Li-H molecule with 1.6 Å distance. The slightly lower value extrapolated from the fit could be due to the non-isolated nature of this molecule inside the $Li_{12}C_{60}$ lattice which manifests itself in a different charge on the Li atom. It is also interesting to notice how ν_Q does not vary significantly on increasing the temperature, indicating that the electric field gradient on lithium, which is affected by its environment, does not undergo major changes during the phase transition, as expected.

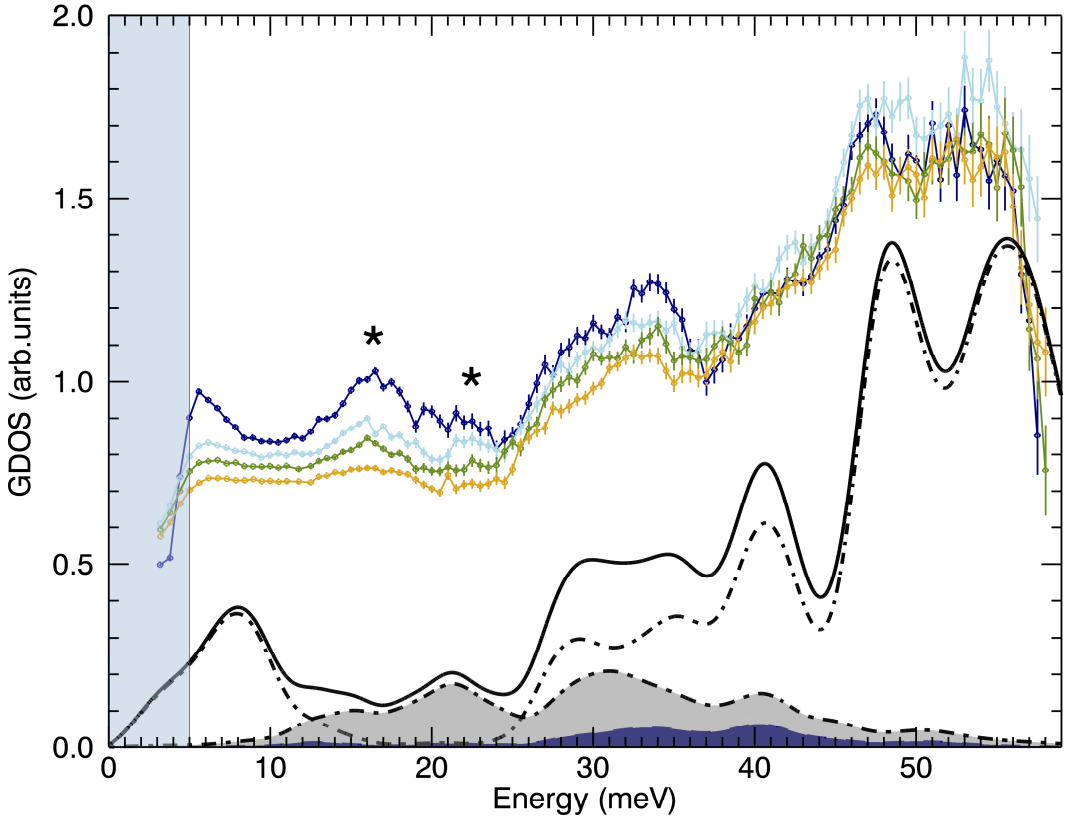

Figure 5: (top curves, from top to bottom, curves are shifted by 0.01 GDOS unit for clarity) Generalized density of states (GDOS) of $Li_{12}C_{60}$ derived from IN4C data using 1.1 Å incident neutrons, as collected at 10, 200, 250 and 320 K. (Bottom curves) Calculated total GDOS of $Li_{12}C_{60}$ (black solid line) and the Carbon (black dot-dashed line) and Lithium (dot-dashed grey area) partial GDOS. The navy area within the grey area represents only the partial GDOS of Li atom at the centre of the tetrahedral cluster. Calculated spectra were convoluted with a Gaussian function having a full width at half maximum matching the energy resolution of the spectrometer.

4. Conclusions

$Li_{12}C_{60}$ system was studied by means of muon spin relaxation spectroscopy and Inelastic Neutron Scattering. Muons stopping in the sample can be separated into two different species: one shows a slow Gaussian relaxation, while the other displays an oscillation. The former is assigned to positive muons, trapped inside the tetrahedral Li clusters located in the pseudo-tetrahedral void of the structure. These muons are particularly sensitive to the Li dynamics and allowed us to highlight the phase transition occurring at high temperature and involving the Li-cluster rearrangement. This

process was also followed by INS, suggesting that above 150 K the Li cluster in $Li_{12}C_{60}$ undergoes a progressive melting, compatible with Li ion diffusion. The second oscillating fraction was assigned to the formation of a covalent Li-Mu species. The trapping of the Mu by the Li ions is the process which reproduces the first step of the hydrogen absorption, just after the H_2 dissociation operated by the Li cluster [15]. The amplitude of the precessing fraction increases on lowering the temperature, which, similarly to Li_6C_{60}, proves that Mu (H) chemisorptions is enhanced at low temperature. On the other hand, Mu behaves quite differently in Li_6C_{60} and $Li_{12}C_{60}$. In the first case, the formation of a muonic radical is observed, proving that H (Mu) is immediately chemisorbed by C_{60} after the molecule dissociation. In the second case, H will bind to Li to initiate the formation of LiH (always found in $Li_{12}C_{60}H_y$) [10]. Only after the amount of free Li in the lattice is suitably decreased, the C_{60} hydrogenation is expected to start. As $Li_{12}C_{60}$ is known to chemisorb hydrogen starting at mild conditions (up to 70 °C) [10], we can deduce that the presence of C_{60} dramatically reduces the temperature (and pressure) necessary to combine H_2 and Li to form LiH. The two factors enhancing Li hydrogenation are: 1- the formation of small Li clusters, 2- their partial ionization. What is the dominant factor is now difficult to anticipate, a more detailed study with increasing Li stoichiometry (now in progress) will help to fully understand the hydrogen absorption mechanism and will allow the engineering of more efficient hydrogen storage materials.

Acknowledgements

The authors would like to acknowledge the financial support from the Cariplo foundation (Project number 2013-0592, “Carbon based nanostructures for innovative hydrogen storage systems). For the μSR experiment, this project has received funding from the European Union's 7th Framework Programme for research, technological development and demonstration under the NMI3-II Grant number 283883. We would also like to acknowledge Dr. Francis Pratt for the technical support during the μSR experiment. Finally, we acknowledge the ILL for inelastic neutron scattering beam time and ILL CS group for free access to clusters.

References

[1] Schlapbach L, Züttel A. Hydrogen-storage materials for mobile applications. Nature 2001;414:353–8. doi:10.1038/35104634.

[2] Züttel A, Sudan P, Mauron P, Kiyobayashi T, Emmenegger C, Schlapbach L. Hydrogen storage in carbon nanostructures. Int J Hydrogen Energy 2002;27:203–12. doi:10.1016/S0360-3199(01)00108-2.

[3] Yoon M, Yang S, Wang E, Zhang Z. Charged fullerenes as high-capacity hydrogen storage media. Nano Lett 2007;7:2578–83. doi:10.1021/nl070809a.

[4] Sun Q, Jena P, Wang Q, Marquez M. First-principles study of hydrogen storage on Li12C60. J Am Chem Soc 2006;128:9741–5. doi:10.1021/ja058330c.

[5] Chandrakumar KRS, Ghosh SK. Alkali-metal-induced enhancement of hydrogen adsorption in C60 fullerene: an ab Initio study. Nano Lett 2008;8:13–9. doi:10.1021/nl071456i.

[6] Sun Q, Wang Q, Jena P, Kawazoe Y. Clustering of Ti on a C60 surface and its effect on hydrogen storage. J Am Chem Soc 2005;127:14582–3. doi:10.1021/ja0550125.

[7] Teprovich JA, Wellons MS, Lascola R, Hwang S-J, Ward P a, Compton RN, et al. Synthesis and characterization of a lithium-doped fullerane (Li(x)-C60-H(y)) for reversible hydrogen storage. Nano Lett 2012;12:582–9. doi:10.1021/nl203045v.

[8] Mauron P, Remhof A, Bliersbach A, Borgschulte A, Züttel A, Sheptyakov D, et al. Reversible hydrogen absorption in sodium intercalated fullerenes. Int J Hydrogen Energy 2012;37:14307–14. doi:10.1016/j.ijhydene.2012.07.045.

[9] Knight DA, Teprovich JA, Summers A, Peters B, Ward PA, Compton RN, et al. Synthesis, characterization, and reversible hydrogen sorption study of sodium-doped fullerene. Nanotechnology 2013;24:455601. doi:10.1088/0957-4484/24/45/455601.

[10] Mauron P, Gaboardi M, Remhof A, Bliersbach A, Sheptyakov D, Aramini M, et al. Hydrogen Sorption in Li 12 C 60. J Phys Chem C 2013;117:22598–602. doi:10.1021/jp408652t.

[11] Yildirim T, Zhou O, Fischer JE, Bykovetz N, Strongin RA, Cichy MA, et al. Intercalation of sodium heteroclusters into the C60 lattice. Nature 1992;360:568–71. doi:10.1038/360568a0.

[12] Rosseinsky MJ, Murphy DW, Fleming RM, Tycko R, Ramirez AP, Dabbagh G, et al. Structural and electronic properties of sodium-intercalated C60. Nature 1992;356:416–8. doi:10.1038/356416a0.

[13] Riccò M, Belli M, Pontiroli D, Mazzani M, Shiroka T, Arčon D, et al. Recovering metallicity in A4C60: The case of monomeric Li4C60. Phys Rev B 2007;75:081401. doi:10.1103/PhysRevB.75.081401.

[14] Giglio F, Pontiroli D, Gaboardi M, Aramini M, Cavallari C, Brunelli M, et al. Li12C60: A lithium clusters intercalated fulleride. Chem Phys Lett 2014;609:155–60. doi:10.1016/j.cplett.2014.06.036.

[15] Aramini M, Gaboardi M, Vlahopoulou G, Pontiroli D, Cavallari C, Milanese C, et al. Muon spin relaxation reveals the hydrogen storage mechanism in light alkali metal fullerides. Carbon N Y 2014;67:92–7. doi:10.1016/j.carbon.2013.09.063.

[16] Tomaselli M, Meier BH, Riccò M, Shiroka T, Sartori A. A multiple-quantum nuclear magnetic resonance study of interstitial Li clusters in LixC60. J Chem Phys 2001;115:472. doi:10.1063/1.1377014.

[17] Cristofolini L, Riccò M, De Renzi R. NMR and high-resolution x-ray diffraction evidence for an alkali-metal fulleride with large interstitial clusters: Li12C60. Phys Rev B 1999;59:8343–6. doi:10.1103/PhysRevB.59.8343.

[18] Pratt F. WIMDA: a muon data analysis program for the Windows PC. Phys B Condens Matter 2000;289-290:710–4. doi:10.1016/S0921-4526(00)00328-8.

[19] Delley B. An all-electron numerical method for solving the local density functional for polyatomic molecules. J Chem Phys 1990;92:508. doi:10.1063/1.458452.

[20] Perdew JP, Burke K, Ernzerhof M. Generalized Gradient Approximation Made Simple. Phys Rev Lett 1996;77:3865–8. doi:10.1103/PhysRevLett.77.3865.

[21] Rols S, Jobic H, Schober H. Monitoring molecular motion in nano-porous solids. Comptes Rendus Phys 2007;8:777–88. doi:10.1016/j.crhy.2007.07.007.

[22] Blöchl PE. Projector augmented-wave method. Phys Rev B 1994;50:17953–79. doi:10.1103/PhysRevB.50.17953.

[23] Kresse G. Efficient iterative schemes for ab initio total-energy calculations using a plane-wave basis set. Phys Rev B 1996;54:11169–86. doi:10.1103/PhysRevB.54.11169.

[24] K. Parlinski. software PHONON. Http://wolf.ifj.edu.pl/phonon/ 2008.

[25] Kubo R. A stochastic theory of spin relaxation. Hyperfine Interact 1981;8:731–8. doi:10.1007/BF01037553.

[26] Hayano R, Uemura Y, Imazato J, Nishida N, Yamazaki T, Kubo R. Zero-and low-field spin relaxation studied by positive muons. Phys Rev B 1979;20:850–9. doi:10.1103/PhysRevB.20.850.

[27] Schenck A. Muon spin rotation spectroscopy: Principles and applications in solid state physics. © Adam Hilger Ltd; 1985.

[28] Celio M, Meier PF. Exact calculation of the muon polarization function. Hyperfine Interact 1984;18:435–40. doi:10.1007/BF02064849.

[29] Meier PF. Spin relaxation of positive muons due to dipolar interactions. Hyperfine Interact 1984;18:427–33. doi:10.1007/BF02064848.

[30] Cottrell SP, Lord JS, Williams WG. Muon charge state and dynamics in the alkali metal hydrides. Phys B Condens Matter 2000;289-290:570–3. doi:10.1016/S0921-4526(00)00259-3.

[31] Williams WG, Brown SR, Cottrell SP. Muon implantation in alkali metal hydrides. Hyperfine Interact 1997;106:105–10. doi:10.1023/A:1012625504691.

[32] MacFarlane W, Kiefl R, Dunsiger S, Sonier J, Chakhalian J, Fischer J, et al. Muon-spin-relaxation studies of the alkali-fulleride superconductors. Phys Rev B 1998;58:1004–24. doi:10.1103/PhysRevB.58.1004.

[33] Chen Y-L, Huang C-H, Hu W-P. Theoretical study on the small clusters of LiH, NaH, BeH(2), and MgH(2). J Phys Chem A 2005;109:9627–36. doi:10.1021/jp051978r.